J Solid State Electrochem (1998) 2: 328–333

ORIGINAL PAPER

L. Sánchez · J.L. Tirado · C. Pérez Vicente · J.C. Jumas

Electrochemical lithium and sodium intercalation into $TaFe_{1.25}Te_3$

Received: 14 October 1997 / Accepted: 14 November 1997

Abstract Lithium and sodium have been topotactically inserted in the lattice of $TaFe_{1.25}Te_3$ by electrochemical procedures. The existence of electronically unequivalent sites occupied by tellurium atoms conditions a two-step insertion process. In each step, the alkali metal ions occupy empty sites in the structure which are coordinated by tellurium atoms of a different set of sites. The thermodynamic and kinetic parameters of $Li_xTaFe_{1.25}Te_3$ and $Na_xTaFe_{1.25}Te_3$ have been determined and compared with other inserted binary and ternary chalcogenides. The values of the free energy of intercalation are less negative than those previously reported for $TaTe_2$ and close to those found for the misfit layer compound $(PbS)_{1.13}TaS_2$. The values of alkali metal ion diffusivity are closer to those reported for the binary telluride, due to the similarities in the atoms exposed to the interlayer space.

Key words Tantalum iron telluride · Alkali metal intercalation · Lithium, sodium battery · Lithium, sodium insertion · Electrochemical intercalation reaction

Introduction

Electrochemical studies have effectively contributed to a detailed understanding of alkali metal intercalation reactions in solids of different composition and structure. In addition, electrochemical procedures allow the synthesis of new compounds, with a better control over the stoichiometry, by allowing known amounts of charge to pass through the electrochemical cell. Moreover, some compounds that were thought to be less prone to intercalation of alkali metals by chemical procedures, such as the *n*-butyllithium technique, provided recent examples of electrochemical insertion reactions, e.g. lithium and sodium intercalation into group five transition metal ditellurides. A particularly outstanding property of these solids is the short distances between the metal atoms in the structure, which can be interpreted in terms of true metal-metal bonds. In fact, bonding in some of these solids has been interpreted as consisting of extended homo- and heterometallic clusters sandwiched between chalcogen atom layers [1, 2]. Moreover, interlayer interactions are also present in some of these solids. These in turn give little significance to a simple 2-D model to describe their layered structures. Both the chalcogen-chalcogen and metal-metal interactions are affected by the changes in electron count induced by the insertion of electron-donating species [3, 4].

The electrochemical intercalation of alkali metals into several ternary chalcogenides with 2-dimensional host lattices has also been studied, particularly for transition metal phosphotrichalcogenides [5] and misfit layer compounds [6, 7]. Because of the structural complexity of some of these systems, some aspects of their intercalation chemistry remain yet unclear. The number of known phases of ternary transition metal tellurides is continuously increasing. The synthesis and structural characterization of solids with MA_xTe_2 (M = Nb, Ta; A = Si, Ge) compositions have been reported [8, 9]. Their structures are not simply derived from that of MTe_2, since M is within a trigonal prismatic environment of Te atoms, and A atoms adopt a very unusual square planar coordination defined by Te atoms in the common face of two connected trigonal prisms.

Recently, the structure of a ternary telluride, $TaFe_{1+x}Te_3$, was reported [10], in which an unusual Ta-Fe bonded network was observed. The lattice of this solid was found to be different from typical layered chalcogenides, which are commonly defined by metal atoms occupying interstices between consecutive close-

L. Sánchez · J.L. Tirado (✉)
Laboratorio de Química Inorgánica, Facultad de Ciencias, Universidad de Córdoba, Avda. San Alberto Magno s/n, E-14004 Córdoba, Spain

C.P. Vicente · J.C. Jumas
Laboratoire de Physicochimie des Matériaux Solides, Université Montpellier II, Place E. Bataillon, F-34095 Montpellier Cedex 5, France

packed chalcogen layers. The proclivity to form metal-metal bonds leads to an unusual Ta-Fe-Fe-Te ribbon network in the structure of this solid. Additional complexity of the framework results from the presence of a partially occupied iron site. Here we examine the insertion of lithium and sodium into this novel host lattice by use of electrochemical techniques.

Experimental details

Submillimeter crystals of the solid with composition $TaFe_{1.25}Te_3$ were obtained by direct synthesis from the elements, in the appropriate proportion, heated to 775 °C [3].

Energy dispersive X-ray microanalysis (EDXMA) was carried out with a JEOL JSM6300 scanning electron microscope. The powder X-ray diffraction (XRD) measurements were performed on a Siemens D-5000 X-ray diffractometer using CuK_α radiation and graphite monochromator. Transmission electron microscopy images and electron diffraction patterns were obtained with a JEOL 200CX microscope.

Electrochemical studies were carried out in two-electrode cells. The electrolyte used was 1 M $LiClO_4$, previously dried under vacuum at 170 °C for 16 h in distilled ethylene/propylene carbonate (1:1 mixture). The telluride electrode pellets (7-mm diameter) were prepared by compressing, at 10 ton $\cdot$ cm^{-2}, ca. 3 mg of active material with PTFE (5 wt%), graphite (7.5 wt%) and acetylene black (7.5 wt%) on a steel grid. Lithium foil was cut into 7-mm diameter circles and was used as the anode vs the telluride electrode. Unless otherwise specified, the cells were cycled galvanostatically with 0.5 mA $\cdot$ cm^{-2} current densities, which were controlled by a MacPile II potentiostat-galvanostat. Step potential electrochemical spectroscopy (SPES) spectra were recorded in 20-mV-steps of 1-h duration.

Results and discussion

The unit cell parameters derived from XRD patterns of the as-prepared telluride powders agree well with previously reported data for a $TaFe_{1.25}Te_3$ stoichiometry [10] (a = 7.416(9) Å, b = 3.628(2) Å, c = 10.011(9) Å, β = 109.01(9)°, V = 269 Å^3). The low-angle reflections found in previous studies for iron contents lower than 1.25 and higher than 1.29, which are indicative of second phases, were absent for our sample. Semiquantitative EDXMA data (Ta = 27.7%, Fe = 11.4%, Te = 60.9%) were also consistent with this composition (calculated for $TaFe_{1.25}Te_3$: Ta = 28.6%, Fe = 11.0%, Te = 60.4%). The electron diffraction patterns recorded in the $\langle 001 \rangle_m$ and $\langle 100 \rangle_m$ zones revealed the basic *hk0* and *0kl* spots, respectively, corresponding to the monoclinic $P2_1/m$ structure.

Figure 1A gives (a) the quasi-equilibrium voltage values (OCV) and (b) continuous galvanostatic discharge data at 0.05 mA $\cdot$ cm^{-2} for each composition of lithium and sodium cells using $TaFe_{1.25}Te_3$ as active cathode material. As usually found in other intercalation electrodes, cell voltages are higher for lithium than for sodium when measured for the same composition and under similar experimental conditions. Similarly, cell voltages are lower when recorded under continuous galvanostatic conditions (Fig. 1B). Also, a complex discharge behavior of the cells is evidenced by the presence of successive regions in the voltage of the cells, which may be associated with energetically different processes of insertion of lithium or sodium ion plus electron. The less steep regions in the OCV plots are commonly associated with well-defined peaks in the corresponding plots of cell current vs x obtained by SPES (Fig. 1B). Thus, for the electrochemical insertion of both alkali metals, two steps are clearly resolved in the different plots of Fig. 1. After the initial drop in voltage and below $x \approx 0.4$, the OCV shows a region in which the voltage decreases smoothly with a limited slope. This effect is evidenced by a low-intensity band which is particularly well resolved for lithium in the SPES plots of Fig. 1B. Following the minima in absolute intensity at ca. x = 0.35, a second less steep

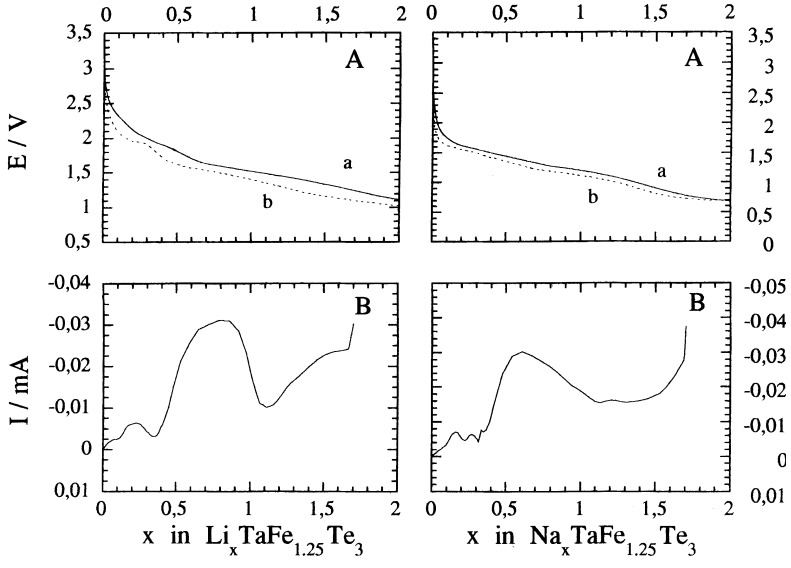

Fig. 1A, B Electrochemical lithium and sodium insertion into $TaFe_{1.25}Te_3$. **A**: *a* Quasi-equilibrium OCV data and *b* continuous galvanostatic discharge at 0.05 mA $\cdot$ cm^{-2}. **B**: Cell current vs composition obtained by SPES

region is observed in the OCV data, which extends up to $x \approx 1.1$, which corresponds also with well-defined bands in the capacity plots with capacity maxima at ca. 0.8 for lithium and 0.6 for sodium. Both signals lead to a slow relaxation of cell current in the vicinity of the peaks, which is characteristic of a slow diffusion of lithium and sodium ions in the host lattice. This behavior is particularly evident in the kinetic plots of Fig. 2.

Additional evidence for the fact that the first two steps in the discharge are a topotactic insertion of lithium and sodium was obtained by recording the XRD and electron diffraction patterns of cathode materials prepared by interrupting the discharge experiments at different depths of discharge below $x = 1.5$. For the $MTaFe_{1.25}Te_3$ compositions, the monoclinic unit cell parameters were $a = 7.421(8)$ Å, $b = 3.62(1)$ Å, $c = 9.99(1)$ Å, $\beta = 108.9(1)°$, $V = 269$ Å^3 for M = Li, and $a = 8.195(8)$ Å, $b = 3.634(4)$ Å, $c = 10.93(1)$ Å, $\beta = 108.81(8)°$, $V = 308$ Å^3 for M = Na. The limited changes in the unit cell parameters, particularly for lithium intercalation, can be associated with both the small size of Li^+ ions and the open structure of the tantalum iron telluride. As discussed above, the interlayer contacts in $TaFe_{1.25}Te_3$ (closest interlayer distance 3.742 Å) are significantly larger than those observed in $TaTe_2$ (closest interlayer distance 3.595 Å). For the same composition, $x = 1$, the electron diffraction data (Fig. 3) were also indexable in the $P2_1/m$ space group as a result of the topotactic nature of the process. The surface of the particles showed a complex topography near the edges, probably as a result of the strains induced by the introduction of lithium and sodium into the interlayer space. The presence of two peaks in the intensity curve, with a minimum for the intermediate composition with $x \approx 0.33$, may be correlated to the formation of two intermediate phases with different compositions and ordered structures resulting from a partial filling of the sites allowable for intercalation. The good correspondence between the composition limits of these intermediates found by OCV and by potentiostatic methods gives additional support to this interpretation. However, the possible occurrence of intermediate phases that could explain the complexity of the cell discharge was not shown by the XRD data of samples obtained at different depths of discharge. It should be noted that direct observation of an ordered lithium lattice is complicated by the relatively small scattering section of lithium and sodium as compared with Ta, Te and Fe atoms. The fractional compositions defining possible intermediates in $M_xTaFe_{1.25}Te_3$ can be deduced from the structural data reported by Li et al. [10]. Accordingly, two types of empty pseudo-octahedral sites between corrugated sandwiches can be distinguished in the $P2_1/m$ structure. The sites defined by Te atoms bridging adjacent Ta-Fe-Fe-Ta ribbons are more favored energetically than those formed by Te directly coordinating the metal ribbons. Thus, the filling of the more favorable but less abundant sites should take place first, followed by the complete filling of the interlayer space for $x \approx 1$ in the second step.

The evaluation of the maximum capacity of these cells was assessed by extended galvanostatic discharge (Fig. 4a). For $x > 1.5$, an extended plateau is observed in Fig. 4a. Cell voltages close to 0.9 V for lithium and 0.6 V for sodium are basically unchanged up to x values close to 10. The presence of such an extended region has also been observed in other layered chalcogenides containing tantalum in their composition. For the misfit

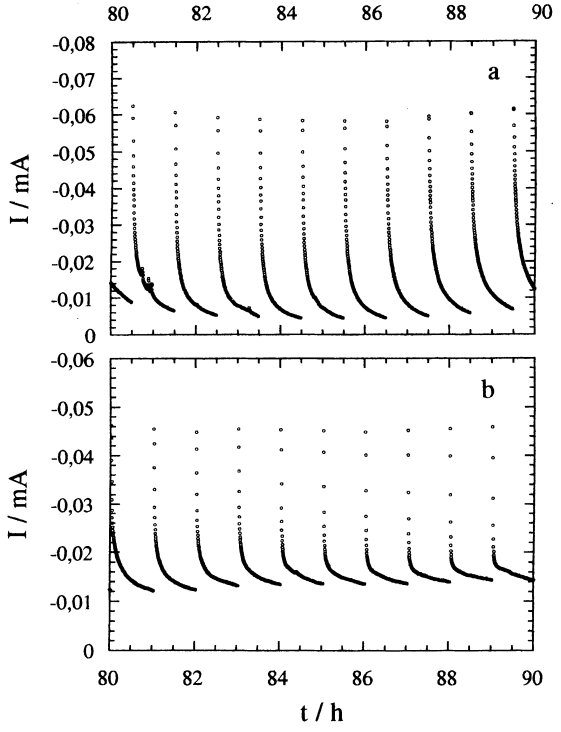

Fig. 2a, b Current relaxation for selected SPES steps in the vicinity of x = 1: *a* lithium cell and *b* sodium cell

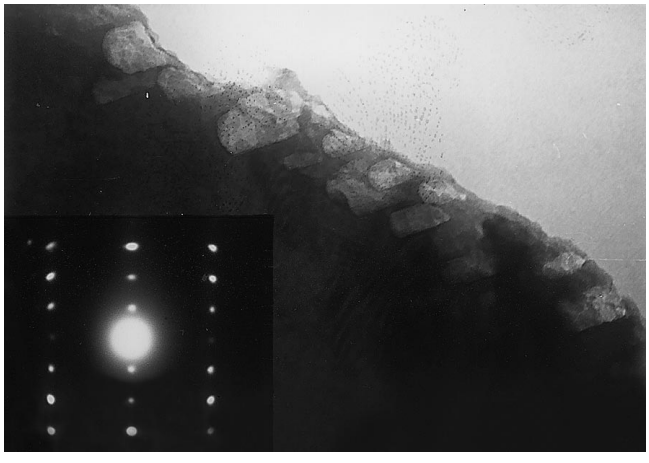

Fig. 3 Bright field image of $LiTaFe_{1.25}Te_3$. Inset: ⟨001⟩ zone axis electron diffraction

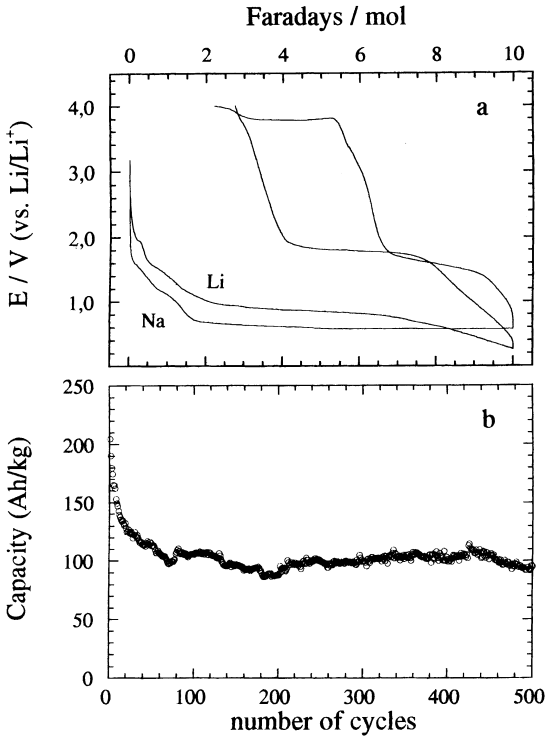

Fig. 4 **a** Extended galvanostatic discharge-charge profile of lithium and sodium cells, and **b** capacity of the lithium cell vs number of cycles. Current density for both plots was 0.05 mA · cm^{-2}

layer compound $(PbS)_{1.14}(TaS_2)_2$ [6], large gravimetric capacities were found in lithium cells irrespective of the large molecular weight of this solid. The observed capacities were mainly due to an extended plateau at ca. 1.2 V. The differences in the cell voltage are indicative of a different process in each case.

The X-ray and electron diffraction data of the cathode materials after the extended plateau reveal a significant loss of long-range ordering, which allows us to regard the electrochemical reaction responsible for the extended plateau as a result of the amorphization of the host matrix. Indirect evidence of this interpretation comes from the enhanced hysteresis found in the discharge-charge V vs x curves recorded by allowing maximum Faraday yields (Fig. 4a), in which charge voltages are close to 1.9 V. It is also worth noting that the diffraction data corresponding to a sample after the first complete galvanostatic cycle showed a significant recovery of crystallinity of the samples. Similar behavior was also found in misfit layer compounds [6, 7]. However, better cycling behavior was found on limiting the capacity to ca. 100 mAh/g. This value is comparable to that found in other electrodes of commercial lithium ion cells. An excellent capacity retention is observed after 500 cycles (Fig. 4b). Although cell voltages are low enough to restrict the practical use of this solid as cathode material, its use as anode material vs 3 or 4 V cathodes could be appropriate in rocking-chair systems. Nevertheless, the search for inexpensive and more environmentally friendly components of cells for large-scale use

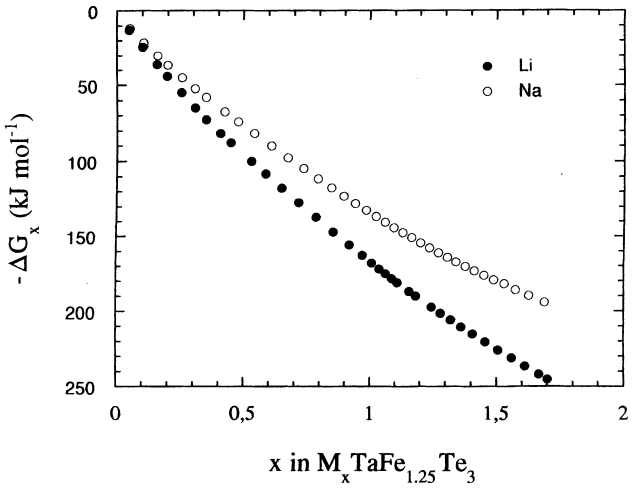

Fig. 5 Plot of standard Gibbs free energy of intercalation vs composition

may restrict its application to cases in which extended cycling is the main objective.

Irrespective of the good cycling properties and large capacities of the host matrix, the study of the thermodynamic and kinetic properties of alkali metal insertion into $TaFe_{1.25}Te_3$ was restricted to depths of discharge below 1.7 F/mol. In fact, further reaction is not a topotactic intercalation but a multiphase decomposition into amorphous products, as discussed above.

The standard Gibbs free energy of lithium and sodium insertion into $TaFe_{1.25}Te_3$ was evaluated as a function of composition by integration of open-circuit voltage vs composition curves, according to the following expression [8]:

$$\Delta G^\circ = -F \int_0^x E \, dx \tag{2}$$

which is simply Faraday's constant times the area under the voltage-composition curve from the pure chalcogenide to the intercalated compound. These results were obtained from the open-circuit voltage measurements included in Fig. 1. Special care was taken to avoid the passage of significant amounts of electricity that could result in some electrical energy dissipation as Joule heat in the internal resistance of the cell during the measurements. Under these conditions, the measured voltages can be considered to be equivalent to e.m.f. values and can be used to obtain ΔG°. The ΔG° values for lithium and sodium intercalation are plotted against x in Fig. 5. The lithium intercalated compounds have more negative standard free energies of intercalation than do the sodium intercalated compounds, which is consistent with the general trend of the free energy of intercalation of alkali metals in transition dichalcogenides [11–13]. If these values are compared with those corresponding to other binary and ternary compounds (Table 1), the following conclusions can be drawn:

Table 1 Values of $\Delta G°$ at 25 °C of the intercalation reaction: $M^+ + e^- + [H] \rightarrow M[H]$ expresssed as kJ/mol, and chemical diffusion coefficients of lithium and sodium ions for different binary and ternary host compounds with layered structure

[H] in M[H]	$\Delta G°$ (M = Li)	$D_{Li}/cm^2\ s^{-1}$	$\Delta G°$ (M = Na)	$D_{Na}/cm^2\ s^{-1}$
TiS_2	−240.3 [12]	$5.0 \cdot 10^{-9}$ [13]	−202.3 [11]	10^{-9} [11]
TaS_2	−211.4 [11]	$(1.5 \cdot 10^{-8})$ [13][a]	−179.5 [13]	$(3.1 \cdot 10^{-8})$ [11][a]
$TaTe_2$	−180.5 [4]	$4.3 \cdot 10^{-9}$ [4]	−156.3 [4]	$1.8 \cdot 10^{-8}$ [4]
$(PbS)_{1.13}TaS_2$	−169.0 [7]	$(2 \cdot 10^{-11})$ [7][a]		
$(PbS)_{1.14}(TaS_2)_2$	−232.5 [16]	$1.8 \cdot 10^{-10}$ [16]	−169.4 [16]	$2.0 \cdot 10^{-10}$ [16]
$TaFe_{1.25}Te_3$	−167.8[b]	$2.8 \cdot 10^{-9}$ [b]	−136.7[b]	$1.5 \cdot 10^{-9}$ [b]

[a] The values in parentheses are average values for intermediate compositions
[b] this work

– As found in binary dichalcogenides, tellurides are thermodynamically less prone to intercalation than sulfides, probably because of the higher covalency in the tellurium-metal bonds and the presence of Te-Te interactions. The reference dichalcogenide, titanium disulfide, displays the highest values for either lithium or sodium intercalation.

– For $TaFe_{1.25}Te_3$, the values of $\Delta G°$ are less negative than for $TaTe_2$, probably as a consequence of the lower average oxidation state of tantalum in the former compound.

– The observed $\Delta G°$ value for lithium is close to that previously found for the misfit layer compound $(PbS)_{1.13}TaS_2$, in which the interlayer space is defined between PbS and TaS_2 layers, the former exposing metal atoms to the interface. On the contrary, for the $(PbS)_{1.14}(TaS_2)_2$ composition, where true TaS_2-TaS_2 interlayers are found, the Gibbs free energy decreases more dramatically. These results agree with the structural model proposed for $TaFe_{1.25}Te_3$, in which Fe atoms of the Ta-Fe-Fe-Ta ribbons are exposed to the interlayer space.

Finally, Fig. 6 shows a comparison of the diffusion coefficients of lithium and sodium insertion into $TaFe_{1.25}Te_3$. These were determined from SPES current-time data plots such as those included in Fig. 2. At long relaxation times the current decays exponentially to zero, and D can be determined from the slope of the $\ln(I)$ vs time plot if the condition $t \gg L/D$ is fulfilled (L: length of the diffusion path ascribed to the thickness of the pellet), according to the following expression [14]:

$$I(t) = 2QDL^2\exp[\pi^2 Dt/(4L^2)] \quad (3)$$

The results in Fig. 6 show significant discontinuities in the values of the diffusion coefficients as a function of composition that may be indicative of the different sites available for intercalation. Several models have been successfully applied to explain the variation of the diffusion coefficients with composition in intercalation compounds. Thus, the model proposed by Nagelberg [15] explains the compositional variation of the diffusion coefficients in binary dichalcogenides with layered 1T and 2H basic structures. For the distorted 1T structure of MTe_2 (M: V, Nb and Ta), it was found that the distorted octahedral sites are not energetically equivalent, and the complexity of the sequence frequencies increases dramatically [4]. For $TaFe_{1.25}Te_3$, the plots in Fig. 1 can be interpreted in terms of the presence of two energetically non-equivalent sites in the interlayer, depending on the presence of iron atoms close to the intercalation sites. A minimum in the D values is found for x values of ca. 0.5 of both lithium and sodium, probably indicating the switch of alkali ion transport from the most favourable set of vacant sites to the other. For $x > 1$, the increase in the D values found for Li intercalation is probably indicative of a more profound change in the mechanism of ion transport, probably as a consequence of the progressive amorphization of the solid host.

On the other hand, the values of Li and Na diffusion coefficients are collected in Table 1 for $x = 1$. These values are of the same magnitude as those previously reported for Li and Na intercalation into the binary tantalum ditelluride, which in turn are slightly lower than those corresponding to tantalum disulfide and slightly higher than those found in ternary misfit layer compounds of tantalum. The origin of these divergences is complex, as it depends on the structure of each solid

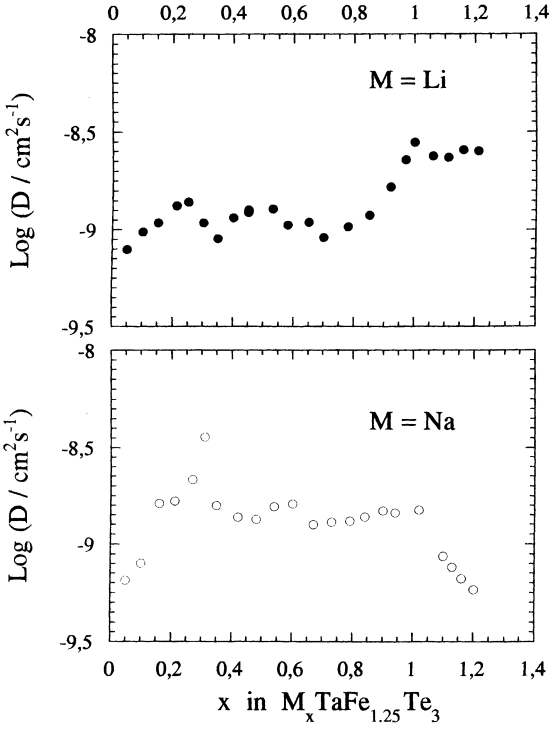

Fig. 6 Plot of coefficients of chemical diffusion of lithium and sodium into $TaFe_{1.25}Te_3$

and the possible interlayer interactions. For $TaTe_2$, Te-Te interlayer distances are short, leading to D_{Li} lower than in TaS_2. For sodium, however, the expansion resulting from sodium intercalation is high and reduces Te-Te interlayer distances. For the misfit layer compounds one has to distinguish between the 1:1:3 and 1:2:5 approximate compositions, in which the complex PbS-TaS_2 interlayers with exposed metal atoms imply poor ionic transport. From this analysis it can be derived that although the Te-Te interactions in $TaFe_{1.25}Te_3$ are not marked (the closest interlayer Te-Te distances are higher than those of $TaTe_2$), this effect is partially compensated by the presence of iron atoms unprotected by the Te layers, and the final D values are comparable to those of the binary compound.

Conclusions

The open structure of the ternary tantalum iron telluride makes it possible to incorporate lithium and sodium topotactically into the empty sites of the lattice up to $MTaFe_{1.25}Te_3$ (M: Li, Na) compositions. Present knowledge about the intercalation properties of two-dimensional compounds is extended to this particular host lattice, in which intermetallic bonds condition the existence of two different environments of Te atoms. Consequently, two steps are found in the electrochemical insertion of alkali metals into Te-coordinated sites, which are evidenced by subtle changes in the slope of the discharge profile. The thermodynamic and kinetic parameters of the intercalation reactions show relevant analogies with the values previously reported for binary and ternary compounds with layered structures. The free energy of intercalation of lithium is similar to that of the ternary misfit layer compound $(PbS)_{1.13}TaS_2$. The main reason for the difference in behavior from that of the binary compound results from the fact that the structure of $TaFe_{1.25}Te_3$ cannot be simply derived from that of $TaTe_2$, and the metal atoms have a lower oxidation state in the ternary iron compound. In contrast, the values of alkali metal ion diffusivity are closer to those reported for the binary telluride, because of the similarities in the atoms exposed to the interlayer space.

Acknowledgements We express our gratitude towards the European Community (Contracts JOU2-CT93-0326 and Training and Mobility of Researchers N° ERBFMBICT 96.0768) and to CICYT (contract PB95-0561) for the financial support for this work.

References

1. Whangbo MH, Canadell E (1992) J Am Chem Soc 114: 9587
2. Canadell E, Jobic S, Brec R, Rouxel J, Whangbo MH (1992) J Solid State Chem 99:189
3. Guzmán R, Morales J, Tirado JL (1994) Inorg Chem 33: 3164
4. Guzmán R, Morales J, Tirado JL (1995) Chem Mater 7: 1171
5. Thompson AH, Whittingham MS (1977) Mater Res Bull 12: 741
6. Hernán L, Morales J, Sánchez L, Tirado JL (1994) Electrochim Acta 39: 2665
7. Lavela P, Morales J, Tirado JL, Bicelli LP, Maffi S (1995) Solid State Ionics 76: 57
8. Li J, Carroll PJ (1992) Mater Res Bull 27: 1073
9. Liang W, Whangbo MH, Evain M, Monconduit L, Brec R, Bengel H, Cantow HJ, Magonov SN (1994) Chem Mater 6: 678
10. Badding ME, Li J, DiSalvo FJ, Zhou W, Edwards PP (1992) J Solid State Chem 100: 313
11. Nagelberg AS, Worrell WL (1979) J Solid State Chem 29: 345
12. Whittingham MS (1978) Prog Solid State Chem 12: 41
13. Basu S, Worrell WL (1977) Symposium on electrode materials and processes for energy conversion and storage. Electrochemical Society, Princeton, p 847
14. Wen CJ, Boukamp BA, Huggins RA, Weppner W (1979) J Electrochem Soc 126: 2258
15. Nagelberg AS (1978) PhD thesis, University of Pennsylvania, Philadelphia, USA, p 127
16. Sánchez L (1994) PhD thesis, University of Córdoba, Spain p 89